

1 **Title:**

2 Climate, CO₂, and human population impacts on global wildfire emissions

3 **Authors:**

4 W. Knorr*¹, L. Jiang & A. Arneth³

5 ¹Physical Geography and Ecosystem Analysis, Lund University, Sölvegatan 12,
6 22362 Lund, Sweden

7 ²National Center for Atmospheric Research, Boulder, Colorado, USA

8 ³KIT/IMK-IFU, Garmisch-Partenkirchen, Germany

9 *Corresponding author's email: wolfgang.knorr@nateko.lu.se

10

11 **Abstract:**

12 Wildfires are by far the largest contributor to global biomass burning and constitute a
13 large global source of atmospheric traces gases and aerosols. Such emissions have a
14 considerable impact on air quality and constitute a major health hazard. Biomass
15 burning also influences the radiative balance of the atmosphere and is thus not only of
16 societal, but also of significant scientific interest. There is a common perception that
17 climate change will lead to an increase in emissions as hot and dry weather events that
18 promote wildfire will become more common. However, even though a few studies
19 have found that the inclusion of CO₂ fertilisation of photosynthesis and changes in
20 human population patterns will tend to somewhat lower predictions of future wildfire
21 emissions, no such study has included full ensemble ranges of both climate
22 predictions and population projections, including the effect of different degrees of
23 urbanisation.

24 Here, we present a series of 124 simulations with the LPJ-GUESS-SIMFIRE global
25 dynamic vegetation – wildfire model, including a semi-empirical formulation for the

26 prediction of burned area based on fire weather, fuel continuity and human population
27 density. The simulations comprise Climate Model Intercomparison Project 5 (CMIP5)
28 climate predictions from eight Earth System Models using two Representative
29 Concentration Pathways and five scenarios of future human population density based
30 on the series of Shared Socioeconomic Pathways (SSPs), sensitivity tests for the
31 effect of climate and CO₂, as well as a sensitivity analysis using two alternative
32 parameterisations of the semi-empirical burned-area model. Contrary to previous
33 work, we find no clear future trend of global wildfire emissions for the moderate
34 emissions and climate change scenario based on the Representative Concentration
35 Pathway (RCP) 4.5. Only historical population change introduces a decline by around
36 15% since 1900. Future emissions could either increase for low population growth
37 and fast urbanisation, or continue to decline for high population growth and slow
38 urbanisation. Only for high future climate change (RCP8.5), wildfire emissions start
39 to rise again after ca. 2020 but are unlikely to reach the levels of 1900 by the end of
40 the 21st century. We find that climate warming will generally increase the risk of fire,
41 but that this is only one of several equally important factors driving future levels of
42 wildfire emissions, which include population change, CO₂ fertilisation causing woody
43 thickening, increased productivity and fuel load, and faster litter turnover in a warmer
44 climate.

45

46 **1 Introduction**

47 Wildfires are responsible for approximately 70% of the global biomass burned
48 annually (van der Werf et al. 2010, updated). Emissions from wildfires in the form of
49 trace gases and aerosols can have a considerable impact on the radiative balance of
50 the atmosphere (Langmann et al. 2009) and also constitute a large source of
51 atmospheric pollutants (Kasischke and Penner 2004). At the same time, wildland fires
52 are an important component of terrestrial ecosystems (Bowman et al. 2009) and the
53 Earth system (Arneth et al. 2010). Fires respond to changes in climate, vegetation
54 composition and human activities (Krawchuk et al. 2009, Pechony and Shindell 2010,
55 Kloster et al. 2012, Moritz et al. 2012), with some model simulations showing a
56 positive impact of climate change on emissions during the 21st century, but a negative,
57 albeit smaller, impact due to changes in land use and increased fire suppression
58 (Kloster et al. 2012).

59 Empirical studies designed at isolating the effect of human population density – here
60 used as an aggregate value representing human interference at the landscape scale –
61 have generally shown that higher population density *per se* leads to a decrease in the
62 annual area burned (Archibald et al. 2008; Knorr et al. 2014; Bistinas et al. 2014),
63 even though there is a common perception that wildfire activity peaks at intermediate
64 levels of population density. This apparent paradox was shown to be the result of co-
65 variations between population density and other factors such as fuel load or
66 flammability - if these co-variations are taken into account, the view of a negative
67 impact is consistent with the observed peak (Bistinas et al. 2014).

68 The main future drivers of changing wildfire have potentially opposing effects on
69 emissions – temperature (increasing), CO₂ via productivity (increasing), CO₂ via
70 woody thickening (Wigley et al., 2010; Buitenwerf et al. 2012; decreasing), and

71 human population density (decreasing emissions). In the meantime, socio-
72 demographic change, interacting with other economic and technological factors, may
73 also lead to climate change – e.g. slow population growth combined with a
74 conventional development pathway of high fossil fuel dependence would result in
75 high CO₂ emissions and large temperature increases. Moreover, the same population
76 growth but with different urbanisation trends could also lead to different levels of
77 spatial population distributions and concentrations, and consequently different results
78 concerning wildfire emissions. Therefore, it is important to first assess the impact of
79 each factor individually before arriving at conclusions concerning aggregate effects.
80 Another important point of consideration is that if climate forcing is based on a model
81 with low climate sensitivity to CO₂ change (i.e. relatively small change in global
82 mean temperature simulated for a given rise in atmospheric CO₂), CO₂ effects might
83 dominate over climate effects. The reverse applies to climate models with a high
84 climate sensitivity. We therefore use an ensemble of climate models instead of only
85 one or two, consider a wide range of future scenarios of population density change,
86 and differentiate between the effects of changes in not only population sizes within a
87 country, but also population spatial distribution via urbanisation.

88 While previous studies have focused on the task of predicting future wildfire
89 emissions and have at most considered impacts of population changes separately to
90 those of climate and CO₂, here we partition the projected changes into the following
91 drivers: climate via changes in burned area, climate via changes in fuel load, CO₂ via
92 changes in burned area, CO₂ via changes in fuel load, and population density
93 considering both the effects of population growth and urbanisation. The goal is a
94 better understanding of the underlying processes of wildfire emission changes, which
95 should help establishing the necessary links between climate policy (emissions),

96 climate science (climate sensitivity), demography, air pollution and atmospheric
97 chemistry, as well as wildfire management.

98 **2 Methods**

99 *2.1 Models and driving data*

100 We use the coupled fire-vegetation model LPJ-GUESS-SIMFIRE (Knorr et al. 2014)
101 to simulate establishment, growth and mortality of natural vegetation, fuel load,
102 burned area and wildfire emissions under changing climate, CO₂ and human
103 population density. LPJ-GUESS (Smith et al. 2001) is a global dynamic vegetation
104 model that simulates potential vegetation as a mixture of user-defined plant functional
105 types (PFTs) which compete with each other in so-called patches. Each PFT is
106 characterized by a set of traits, such as leaf longevity and phenology, growth form and
107 bioclimatic limits to establishment and survival. In these simulations, we use five
108 patches per grid cell, and within each patch, LPJ-GUESS simulates several age
109 cohorts. In "cohort mode", which is used here, all individuals of a cohort are assumed
110 to have identical characteristics. When a fire occurs, individuals of woody PFTs
111 within each patch are selected at random to be killed or to survive according to the
112 PFT's fire resistance (Knorr et al. 2012). Grass PFTs have no individuals and
113 therefore we only adjust the biomass of each these PFTs. We use PFTs designed for
114 global simulations as given by Ahlström et al. (2012).

115 Fire impacts on vegetation are simulated at monthly intervals as described by Knorr et
116 al. (2012). SIMFIRE predicts annual fractional burned area, A (the fraction of each
117 grid cell burned per year) using the following equation:

$$118 \quad A(y) = a(B) F^b N_{max}(y)^c \exp(-ep) \quad (1)$$

119 Here, y is the fire year defined as in Knorr et al. (2012) in such a way that it never
120 "cuts" the fire season in two, B the biome type, F is annual potential fraction of
121 absorbed photosynthetically active radiation (FAPAR), an approximation of
122 vegetation fractional cover easily observed from satellites and here used as a measure
123 of fuel continuity (Knorr et al. 2014), N_{max} is the annual maximum Nesterov Index
124 based on daily diurnal temperature mean, T_m , range, T_r , and precipitation, P , and p is
125 human population density. The Nesterov index used is given by Thonicke et al.
126 (2010) as the cumulative sum of $T_m*(T_r + 4K)$ over all consecutive days with equal or
127 less than 3 mm rainfall. $a(B)$, b , c , and e are global parameters derived by
128 optimisation of SIMFIRE against observed burned area from GFED3 (Giglio et al.
129 2010) on a spatial grid and for the entire globe (Table 2, "GFED3", "All population
130 densities" of Knorr et al. 2014). To derive monthly burned area, we use the average
131 diurnal cycle of burned area derived from GFED3 for 2001-2010 using a variable
132 spatial averaging radius around each grid cell which is at least 250 km but has a total
133 burned area over the period of 10,000 km². Information on biome type is passed from
134 LPJ-GUESS to SIMFIRE, where biome type is a discrete number ranging from one to
135 eight, using FAPAR of woody and herbaceous vegetation and of vegetation of at least
136 2 m as well as geographic latitude as information. F in Eq. (1) is a bias corrected
137 value derived from LPJ-GUESS simulated FAPAR, F_s , via:

$$138 \quad F = 0.42 F_s - 0.15 F_s^2 \quad (2)$$

139 In LPJ-GUESS, woody thickening effects emissions in two ways: When the fraction
140 of shrubs increases, the area belonging to the biome "shrubland" increases relative to
141 the area of the biome "savannah and grassland". Because $a(B)$ of Eq. (1) for the
142 former is approximately half of the value for the latter (Knorr et al. 2014), an increase
143 in the fraction of shrubland immediately leads to a decrease in burned area. The

144 second effect results from the fact that in a fire, 100% of live and dead leaves of
145 grasses burn, while for woody vegetation, 100% of dead leaves but only between 46
146 and 59% of live leaves (depending on fire resistance), 20% of dead wood and no live
147 wood burn in a fire (Knorr et al. 2012). As a result, the fraction of net primary
148 productivity emitted in a fire tends to decrease with woody encroachment. The
149 measure used to document woody thickening in LPJ-GUESS is the maximum
150 seasonal leaf area index (LAI) assigned the woody individuals of a grid cell divided
151 by the total grid cell LAI.

152 LPJ-GUESS-SIMFIRE, in the following denoted "LPJ-GUESS", is driven by output
153 from Earth system model (ESM) simulations from the CMIP5 project (Taylor et al.
154 2012) in a way mostly following Ahlström et al. (2012), where climate output of
155 monthly mean temperature, precipitation and downward shortwave radiation is bias
156 corrected using the mean observed climate for the period 1961-1990, and atmospheric
157 CO₂ levels used by LPJ-GUESS are taken from the RCP scenarios as prescribed for
158 CMIP5 (Meinshausen et al. 2011). In variance to the cited work, we use CRU TS3.10
159 (Harris et al. 2014) as climate observations, and we predict monthly mean diurnal
160 temperature range and number of wet days per month based on linear regressions
161 against mean temperature and precipitation, respectively. Simulations are carried out
162 on an equal-area pseudo-1° grid, which has a grid spacing of 1°x1° at the equator and
163 a wider E-W spacing towards the poles in order to conserve the average grid cell area
164 across latitude bands.

165 We use global historical gridded values of human population density from HYDE
166 (Klein-Goldewijk et al. 2010) for simulations up to 2005. For future scenarios, no
167 gridded data are available, but we use instead per-country values of total population
168 and percentage of urban population. In order to generate gridded population density

169 after 2005, we use separate urban and rural population density from HYDE for the
170 year 2005 and re-scale both by the relative growth of each in each country. After this
171 procedure, we multiply the population density of all grid cells representing each
172 country by a constant factor such that the growth of the total population of the given
173 country relative to the 2005 HYDE data matches that of the per-country total
174 population scenario used.

175 ***2.2 Scenarios***

176 We run simulations for two climate change scenarios from the Representative
177 Concentration Pathways (RCP). Of these, RCP4.5 represents an approximate radiative
178 forcing scenario typical of the majority of stabilisation scenarios included in the
179 Fourth Assessment of Report of the International Panel on Climate Change. The
180 other, RCP8.5, is a typical case of high emissions resulting from a lack of enforced
181 stabilisation of greenhouse gases, leading to high levels of climate change (van
182 Vuuren et al. 2011). In this study, we will consider both scenarios separately as two
183 alternative futures without any assignment of relative probabilities.

184 Climatic trends simulated for the 20th century as well as for RCP4.5 and RCP8.5 are
185 shown in Table 1 for different regions, for the eight-ESM ensemble mean and range.
186 (For definition of regions see Section 2.4 and Fig. 4.) There is a spatially rather
187 uniform warming trend of around half a °C during the 20th century roughly in
188 accordance with observations (Harris et al. 2014), with inter-model differences larger
189 than differences between regions. Precipitation declines slightly during the same
190 period, most strongly for already dry Middle East, with generally rather large inter-
191 model differences, in particular for Africa, Oceania and South Asia. Temperature
192 change under the RCP4.5 scenario towards the end of the 21st century is around

193 +2.5°C for most regions, except for higher values for the two regions comprising most
194 of the Arctic (North America, North Asia), while precipitation overall increases, albeit
195 with considerable declines for Oceania and Middle East on average, and for South
196 America and Africa for their respective ensemble minima. For RCP8.5, global
197 mean temperature change reaches as high as +5°C, with North America, North Asia
198 and Middle East exceeding this value. Precipitation changes are similar to RCP4.5,
199 but with both the inter-model ranges and the inter-region differences considerably
200 amplified. (For example, there is an almost 40% decline for Oceania for the ensemble
201 minimum.)

202 For population scenarios, we use marker scenarios of the Shared Socioeconomic
203 Pathways (SSPs; O'Neill et al. 2012, Jiang 2014). We consider a total of five
204 scenarios: SSP2 scenario with medium population growth and central urbanisation,
205 two extreme scenarios with either high population growth and slow urbanisation
206 (SSP3) or low population growth with fast urbanisation (SSP5), and two further
207 scenarios in which the medium population growth (SSP2) is combined with either
208 slow (SSP3) or fast (SSP5) urbanisation. For the purpose of analysis, we will consider
209 these five scenarios equally plausible, keeping in mind, however, that this is mainly a
210 working hypothesis.

211 ***2.3 Simulations***

212 We combine output from eight ESMs with two different emissions pathways, one
213 based on RCP4.5 and one on RCP8.5, all run with the medium population and central
214 urbanisation scenario of SSP2. These 16 simulations are repeated six times using the
215 other four population and urbanisation scenarios, one simulation each where
216 population is held constant at 2000 levels, and one simulation where both population
217 and atmospheric CO₂ levels are held constant at 2000 levels, giving $8 * 2 * 7 = 112$

218 simulations. To these we add two more sets of six simulations each with a different
219 parameterisation of SIMFIRE, comprising runs using the SSP2 demographic scenario,
220 fixed population, and fixed population and CO₂ and output from MPI-ESM-LR based
221 on either RCP4.5 or RCP8.5. The first alternative SIMFIRE parameterisation is
222 derived from a global optimisation against MCD45 burned area (Roy et al. 2008)
223 according to Knorr et al. (2014, Table 2, "MCD45", "All population densities"), and
224 the other assumes a slight increase in burned area with increasing population density
225 if p is less than 0.1 inhabitants per km², where Eq. (1) is replaced by:

$$226 \quad A(y) = (0.81 + 1.9p) a(B) F^b N_{max}(y)^c \exp(-ep), \quad (3)$$

227 based on results presented by Knorr et al. (2014).

228 ***2.4 Analytical Framework***

229 Since the present analysis only considers wildfires, we exclude all grid cells that
230 contain more than 50% of cropland at any time during 1901-2100 in either the
231 RCP6.0 or 8.5 land use scenarios (Hurtt et al. 2011). The threshold of 50% is the same
232 as used during SIMFIRE optimisation. A time-invariant crop mask is used in order to
233 avoid introducing time trends in the results through temporal variations of the crop
234 mask. We therefore only consider the indirect effect of cropland expansion via the
235 empirically derived burned area--population density relationship of SIMFIRE, not the
236 direct displacement of wildlands. This indirect effect can be considerable and arises
237 from the fact that cropland expansion tends to be accompanied by higher population
238 density, a denser road network, and a decrease in burned area in the areas that have
239 not been converted to croplands (Andela and van der Werf 2014).

240 The changes in emissions may be caused by climate change alone, by changes in
241 atmospheric CO₂, or by changes in population density. Emissions are determined by

242 the product of burned area, the amount of fuel present, and the fraction of fuel
 243 combusted in a fire. Climate affects burned area directly by changing fire risk via
 244 N_{max} , while climate and CO₂ affect burned area indirectly by changing the vegetation
 245 type, which affects $a(B)$, or vegetation cover, which affects F in Eq. (1). Fuel load is
 246 also affected by vegetation productivity which is driven by both climate and CO₂, and
 247 by litter decay rates, which depend on temperature and precipitation (Smith et al.
 248 2001). The combusted fraction of fuel mainly depends on the presence of grasses vs.
 249 trees (Knorr et al. 2012). Finally, population density affects emissions through burned
 250 area via Eq. (1).

251 In order to assess the effect of different driving factors on changing emissions, we
 252 employ the following analytical framework:

$$253 \quad E_{T2} = E_{T1} + \Delta E, \quad (4a)$$

$$254 \quad E_{T2}^{p2} = E_{T1}^{p2} + \Delta E^{p2}, \quad (4c)$$

$$255 \quad E_{T2}^{cp2} = E_{T2}^{cp2} + \Delta E^{cp2} \quad (4b)$$

256 with

$$257 \quad \Delta E = \Delta E_{\text{clim}} + \Delta E_{\text{CO}_2} + \Delta E_{\text{pop}}, \quad (5a)$$

$$258 \quad \Delta E^{p2} = \Delta E_{\text{clim}} + \Delta E_{\text{CO}_2}, \quad (5b)$$

$$259 \quad \Delta E^{cp2} = \Delta E_{\text{clim}}. \quad (5b)$$

260 where subscript $T1$ denotes the temporal average over the initial reference period
 261 (either 1901-1930 or 1971-2000), and $T2$ over the subsequent reference period (1971-
 262 2000 or 2071-2100), E are wildfire emissions, ΔE the change in the temporal average
 263 of emissions between the two reference periods, and the subscripts "clim", "CO₂" and
 264 "pop" denote the effects of changing climate, CO₂ and human population density,
 265 respectively. The superscripts $p2$ are for the simulations with population density fixed

266 at year 2000 levels, and *cp2* for the simulations with both CO₂ and population fixed at
267 2000 levels. We choose the year 2000 as a reference year for fixed input variables in
268 the middle of the simulation period in order to minimise deviations from the values of
269 the transient runs.

270 The climate effect in the context of this study is therefore defined as the change in
271 emissions between two time periods of a transient simulation with variable climate
272 but fixed population density and atmospheric CO₂, the CO₂ effect as the additional
273 change in emissions when CO₂ is also varied in time, and the population effect as the
274 additional effect when population density also becomes time variant. The computed
275 effects are not expressions of model sensitivity to small perturbations, but rather arise
276 from a series of specific scenarios. We choose this order of scenarios for historical
277 reasons: we first include the effect studied most (e.g. Krawchuk et al., 2009; Moritz et
278 al., 2012), then the effect that is usually included as soon as a dynamic vegetation
279 model is used (Scholze et al. 2006), and at last the effect that is the focus of the
280 current study. If we were to add the population effect first – by including simulations
281 where population changes in time but CO₂ is kept constant – the results would be
282 somewhat different, and the difference could be expressed as interaction terms
283 following Stein and Alpert (1993). However, this method is usually applied to time
284 slice experiments (e.g. Claussen et al. 2001; Martin Calvo and Prentice 2015) and its
285 application to transient simulations is less straightforward, still depends on a finite
286 perturbations, and would require a large number of additional simulations, which is
287 why we here restricted ourselves to the setup described by Eqs. (4) and (5).

288 Fire emissions here are computed as the product of burned area and area-specific fuel
289 combustion. Therefore, we can further subdivide the CO₂ effect on emissions between
290 those that work via changing burned area ($\Delta E_{\text{CO}_2}^{\text{b.a.}}$) and those via changing

291 combustible fuel load as the remainder ($\Delta E_{\text{CO}_2}^{\text{c.f.l.}} = \Delta E_{\text{CO}_2} - \Delta E_{\text{CO}_2}^{\text{b.a.}}$). We derive the
 292 former in a first-order forward projection using emissions per area burned of the
 293 previous time step::

$$294 \quad \Delta E_{\text{CO}_2}^{\text{b.a.}} = \Delta B_{\text{CO}_2} (E_{T1} / B_{T1}) , \quad (6)$$

295 where B_{T1} is the temporal average of burned area during reference period $T1$, and
 296 ΔB_{CO_2} the change in burned area due to CO_2 changes, which we approximate in an
 297 analogous way to ΔE_{CO_2} as:

$$298 \quad \Delta B_{\text{CO}_2} = B_{T2}^{p2} - B_{T1}^{p2} - (B_{T2}^{cp2} - B_{T1}^{cp2}) . \quad (7)$$

299 An analogous formulation is used in order to discern climate impacts due to burned
 300 area from those due to changes in fuel load and its degree of combustion:

$$301 \quad \Delta E_{\text{clim}}^{\text{b.a.}} = \Delta B_{\text{clim}} (E_{T1} / B_{T1}) , \quad (8)$$

302 with

$$303 \quad \Delta B_{\text{clim}} = B_{T2}^{cp2} - B_{T1}^{cp2} . \quad (9)$$

304 We analyse the main driving factors of emissions changes using Eq. 5–9 for selected
 305 large regions, aggregated from the standard GFED regions (Giglio et al. 2010):

- 306 1. North America (GFED Boreal and Temperate North America, Central
 307 America)
- 308 2. South America (GFED Northern and Southern-Hemisphere South America)
- 309 3. Europe (same as GFED)
- 310 4. Middle East (same as GFED)
- 311 5. Africa (GFED Northern and Southern-Hemisphere Africa)
- 312 6. North Asia (GFED Boreal and Central Asia)
- 313 7. South Asia (GFED South-East and Equatorial Asia)
- 314 8. Oceania (GFED Australia and New Zealand)

315 For a probabilistic analysis of changes in emissions, we follow previous work by
316 Scholze et al. (2006), who counted ensemble members driven by differing climate
317 models where the change of the temporal average between two reference periods was
318 more than one standard deviation of the interannual variability of the first reference
319 period. The authors found a general pattern of increasing fractional burned area in arid
320 regions, and a decline at high latitudes and some tropical regions. Here, we apply the
321 method to emissions and use two standard deviations instead in order to ensure that
322 the change is highly significant.

323 **3 Results**

324 *3.1 Global emission trends*

325 Global simulated emissions taking into account changes in all factors, climate, CO₂
326 and population, decline continuously between about 1930 and 2020 for all members
327 of the ESM ensemble (Fig. 1). Thereafter, emissions approximately stabilize, albeit
328 with a very slight upward trend during 2080-2100 for the moderate greenhouse gas
329 concentrations and climate change scenario RCP4.5 and the central demographic
330 scenario (Fig. 1a). However, different demographic scenarios lead to considerable
331 variations in simulated emissions: while emissions continue to decline until 2100
332 under high population growth and slow urbanisation (SSP3), the trend of declining
333 emissions is reversed from around 2010 and emissions will resume current levels by
334 the end of the 21st century under low population growth and fast urbanisation (SSP5)
335 when taking the ESM ensemble mean. In general, higher population growth drives
336 emissions downward (comparing SSP3 to SSP5), while faster urbanisation contributes
337 to higher wildfire emissions (comparing SSP2 population with fast and slow
338 urbanisation). By the end of the century, different demographic trends generate
339 approximately 0.2 GtC per year difference (ranging from around 1.1 to 1.3 GtC/yr)

340 under the moderate climate change RCP4.5. Overall, the range of future emissions
341 spanned by the eight ESMs, but using a single, central population scenario, is less
342 than half of the range spanned by all ESMs and population scenarios combined. None
343 of the simulations see late 21st century emissions reach the levels again that are found
344 for the beginning of the 20th century (Table 2). Only 9 out of 40 simulations show
345 global average emissions during 2071-2100 higher than during 1971-2000, seven out
346 of which are for low population growth and fast urbanisation, and one for
347 intermediate population growth and fast urbanisation.

348 Under RCP 8.5, with high greenhouse gas concentrations and climate change, global
349 wildfire emissions start to rise again after 2020 even for the central demographic
350 scenarios (SSP2) and by the end of the 21st century reach levels only slightly below
351 those of the beginning of the 20th century (Fig. 1b). According to this climate change
352 scenario, the world is currently in a temporary minimum of wildfire emissions,
353 independent of demographic scenario or ESM simulation. The population scenario
354 rather determines when emissions are predicted to rise again and how fast emissions
355 increase. For a scenario of high population growth and slow urbanisation (SSP3),
356 emissions rise again after ca. 2070 and reach about 1.2 GtC/yr by the end of the
357 century, while under the fast urbanisation scenarios (SSP5 and SSP2 population with
358 fast urbanisation), they already start rising around 2020. Under RCP8.5, different
359 demographic trends result in different wildfire emissions ranging from 1.2 to 1.5
360 GtC/yr. Overall, for 28 out of 40 simulations average emissions during 2071-2100 are
361 higher than during 1971-2000, and for three out of the eight simulations with low
362 population growth and fast urbanisation they are even higher than for 1901-1930
363 (Table 2).

364 Simulations with atmospheric CO₂ and population held constant at 2000 levels reveal
365 the impact of climate change on simulated wildfire emissions (Fig. 2a). The climate
366 impact is here shown as the difference in emissions against the average during 1971-
367 2000 (1.28 PgC/yr, see Table 2). There is a modest positive climate impact on global
368 emissions for RCP8.5, which reaches close to 10% towards the end of the 21st century
369 for the ESM ensemble mean, with a range between close to 0 and +20%. For the past,
370 there is no discernable impact of climate change. For RCP4.5, the impact is very
371 small and peaks around 2050 for the ensemble mean, but with a range skewed slightly
372 towards increased emissions.

373 The CO₂ impact is computed as the difference between two simulations with fixed
374 population density, the one with variable climate and CO₂ minus the one with variable
375 climate but fixed CO₂ (Eq. 5). The resulting emissions differences (Fig. 2b) remain
376 negative throughout the historical period until 2005 because the fixed-CO₂
377 simulations start out with considerably higher CO₂ levels than the variable-CO₂ ones
378 leading to higher productivity (CO₂ fertilisation, see Hickler et al. 2008, Ahlström et
379 al. 2012), higher fuel load and therefore higher emissions. For RCP8.5, the global
380 CO₂ impact on emissions is about the same as the climate impact, but for RCP4.5 it is
381 much larger. The magnitude of the CO₂ effect itself is climate dependent, which can
382 be seen by the inter-ensemble range, which is caused solely by differences in climate.
383 (All ensemble members use the same atmospheric CO₂ scenarios for a given RCP.)

384 There is also a small interannual variability caused mainly by climate fluctuations,
385 since interannual variations in atmospheric CO₂ are small until 2005 and absent from
386 the scenarios (Meinshausen et al. 2011). As for climate, there is no discernable CO₂
387 impact on past emission changes.

388 Finally, the demographic impact is simulated by the difference between simulations
389 with time varying climate, CO₂ and population, and the corresponding simulations
390 where population is fixed, but the other two vary with time (Eq. 5). As one would
391 expect, the results for the two RCPs are indistinguishable, with a small climate-related
392 ensemble range and a small amount of interannual variability caused by climate
393 fluctuations (Fig. 2c). The simulated demographic impact for the central population
394 scenario is towards declining emissions mainly driven by population growth. After
395 2050, the effect declines rapidly, and there is a very slight positive trend after ca. 2090
396 which is due to the levelling off of projected population growth (SSP2) and
397 continuing urbanisation. As can be seen by comparing simulated emissions between
398 the central (SSP2) and the remaining population scenarios (Fig. 1a), the demographic
399 impact varies considerably between scenarios, with a continuing negative impact until
400 2100 for the scenario with high population growth with slow urbanisation (SSP3), but
401 a positive impact of the demographic change on global emission trends from about
402 2040 for low population growth with fast urbanisation (SSP5).

403 Results for the set of sensitivity tests where the parameterisation of SIMFIRE was
404 modified are shown in Fig. 3 for the climate, CO₂ and demographic impacts
405 separately. Note that in this case, simulations are performed with only one ESM
406 (MPI-ESM-LR). The climate impact on emissions is again small for RCP4.5, but
407 discernably positive for RCP8.5 after ca. 2020. The climate impact is hardly affected
408 by changing the SIMFIRE parameterisation. The CO₂ effect is similar to the ensemble
409 mean (Fig. 2b), but with a marked decline after ca. 2080 for RCP8.5. In this case,
410 SIMFIRE optimised against MCD45 burned area shows less of a positive trend after
411 2020 as a result of CO₂ changes than the standard formulation, and a more
412 pronounced negative effect after 2080. Also, the simulated historical and future

413 demographic impacts are slightly less for MCD45 than for the standard version. The
414 SIMFIRE version with an initial increase in burned area with population density (Eq.
415 3) has only a very small impact on simulated global emissions.

416 The recent estimate from the GFED4.0s data set puts the average global wildfire
417 emissions at 1.5 PgC/yr (released May 2015, 1997-2014 average of savannah, boreal
418 and temperate forest fires combined, against 2.2 PgC/yr for all biomass burning, van
419 der Werf et al. 2010, updated using Randerson et al. 2012 and Giglio et al. 2013),
420 slightly higher than simulated here (Table 2). During the 20th century, global
421 emissions decrease by around 150 TgC/yr, a little more than 10%. The main driving
422 factor of this decrease is growing population, while climate and CO₂ changes have
423 only a very small impact on emissions, as already discussed with Fig. 2. Further
424 analysis of these driving factors (Fig. 4), however, reveals that this small impact is
425 due to compensating action on either burned area (Eqs. 6 and 8) or combustible fuel
426 load (the remainder). Globally, climate had a small positive and CO₂ a slightly
427 smaller negative effect on emissions via burned area. At the same time, climate had a
428 negative and CO₂ a positive impact on combustible fuel load. For the 21st century
429 (Fig. 5), this constellation is predicted to continue, with a somewhat larger
430 demographic impact that is negative across all ensemble members. The overall effect
431 on emissions, however, is small and of uncertain sign (ensemble range including both
432 positive and negative changes). This is because the climate impact and even more
433 both CO₂ effects, acting in opposite directions, increase several fold compared to the
434 situation during the 20th century.

435 ***3.2 Driving factors of regional emission changes***

436 By the beginning of the 20th century, the main wildfire emitting region is clearly
437 Africa (Fig. 4), followed by South America, North Asia and Oceania. Emission
438 changes towards the end of the 20th century are mainly due to changes in population
439 density in all regions except for Europe, North America and Oceania where
440 population growth rates are significantly lower. For Europe, climate change has led to
441 an increase in burned area, but an about analogous decrease in fuel load, such that the
442 overall climate effect is small and uncertain. The result for North America is similar,
443 while there is a larger but still uncertain positive CO₂ effect on fuel load, similar to
444 Oceania and South America. For Oceania the population effect is by far the smallest
445 and the only one uncertain in sign (judging by the ensemble range).

446 The climate effect via fuel load is negative in all regions, while the climate effect via
447 burned area is almost always positive, except for the Middle East where it is negative
448 but with a large ensemble range spanning both positive and negative, and South Asia,
449 where it is close to zero. We find a negative CO₂ effect via burned area in the tropics
450 (Africa, South America), but a positive effect in the arid sub-tropics and temperate
451 zones (Middle East, North Asia). The positive climate effect can be explained by
452 regional changes in N_{max} (Table 3, cf. Eq. 1), which are always positive, small for
453 changes during the 20th century, but reaching up to over 100% for Europe from the
454 period 1971-2000 to 2071-2100 under the RCP8.5 climate change scenario. The
455 highest increases are for the northern regions, and the smallest for regions with large
456 deserts, like Africa and Middle East, but starting from a high base. However, climate
457 change can also affect burned area indirectly through vegetation change by changing
458 B or F in Eq. (1), for which a good indicator is the fraction of the total leaf area index
459 that is attributed to grasses ("grass fraction", Table 3). This is because $a(B)$ for
460 grassland and savannahs is about one order of magnitude larger than $a(B)$ for woody

461 biomes (Knorr et al. 2014). There is a general increase in the fraction of woody at the
462 expense of grass vegetation across all except the hyper-arid Middle East region. Here,
463 the grass fraction is by far the highest and the climate too dry to support the expansion
464 of shrubs.

465 For 1971-2000, simulated wildfire emissions are markedly lower than for the
466 beginning of the 20th century for Africa, South America, South Asia and Middle East
467 (Fig. 5). Of these regions, only Africa is predicted to continue to decline for the entire
468 ensemble range for both RCPs. The main drivers are population growth and CO₂
469 impact on burned area, partly compensated by increased fuel load. For South
470 America, South Asia and Oceania the pattern is similar, except with a much smaller
471 demographic impact, resulting in an overall change of uncertain direction.

472 All northern regions (North America, Europe and North Asia) are predicted to
473 increase emissions across the entire ensemble. All of these have a slight positive
474 climate impact, but with large uncertainties, where climate change strongly increases
475 burned area compensated largely by a decrease in fuel load. Since precipitation is
476 predicted to increase in these regions (Table 1), the climate effect is mainly due to
477 increasing temperatures and N_{max} (Tables 1, 3). For North America and North Asia
478 there is a clear positive effect of CO₂ on fuel load which appears to be the main
479 reason for tilting the balance towards emission increases. However, population change
480 plays a rather small role, with a large ensemble range for Europe and North Asia
481 making the sign of the impact uncertain given their slower population growth. For
482 North America, the demographic impact is small, but universally slightly negative. An
483 exception is the region Middle East, which has a large positive CO₂ effect via burned
484 area (cf. Fig. 4).

485 Overall, there is a marked shift in emissions towards the extra-tropics: while for 1971-
486 2000, the tropics have 700 TgC/yr emissions vs. 580 for the extra-tropics (ensemble
487 mean), for 2071-2100 the split ranges between 420 tropics vs. 680 extra-tropics for
488 RCP4.5, high population growth / slow urbanisation, and 600 tropics vs. 720 extra-
489 tropics for RCP8.5, low population growth / fast urbanisation. As the regional
490 analysis shows, this change is mainly the result of expanding population in Africa.
491 However, there is also a much stronger negative climate effect on fuel load at high
492 compared to low latitudes (Fig. 6), which to some degree slows down the shift of
493 emissions to the north. This contrasts with a generally positive CO₂ effect across most
494 of the globe, but with about the same magnitude for tropical and extra-tropical
495 vegetated areas. At high latitudes, combustible fuel load is generally much higher than
496 at low latitudes, implying that this is compensated for by a much smaller burned area,
497 leading to overall lower emissions in this region.

498 ***3.3 Probabilistic forecast of future emission changes***

499 For simulated emissions during the 20th century, we find that a majority of ensemble
500 members show significant increases (i.e. by more than two standard deviations) for
501 northern boreal regions and the Tibetan plateau, and decreases for some scattered
502 regions in Europe and China, but in general, changes are small compared to
503 interannual variability (Fig. 7a). For the 21st century, most simulations for both
504 RCP4.5 (Fig. 7b) and RCP8.5 (Fig. 7c) predict a significant decrease in emissions in
505 Africa, mainly north of the equator, and to a lesser degree and mostly for RCP8.5 for
506 North Australian savannahs. The main regions for which a significant increase in fire
507 emissions is predicted are the boreal-forest / tundra transition zones, Europe and
508 China, and arid regions in Central Australia, southern Africa and Central Asia. For the

509 arid regions, however, the increase is much more pronounced for RCP8.5 than for
510 RCP4.5.

511 These changes in fire emissions during the 21st century relative to current variability
512 can also be analysed by driving factor (Eqs. 4 and 5). The analysis reveals that
513 increases in emissions in the boreal/tundra transitional zone are mostly due to climate
514 change, except for the more continental and arid north-eastern Siberia. For the rest of
515 the globe, the climate effect has a surprisingly small impact, being confined to narrow
516 bands of arid regions in southern Africa, Australia and the Arabian Peninsula. Climate
517 change also leads to a significant decrease in emissions in northern Africa and the
518 Middle East (Fig. 8a-b, cf. Fig. 5). For RCP4.5, CO₂ has only a small positive impact
519 on emissions, mainly for Central Asia, and a negative impact for African, South
520 American and North Australian tropical savannahs. For RCP8.5, the CO₂ effect has a
521 much bigger impact globally on the relative change of emissions, leading to increased
522 emissions in large regions including Mexico, southern South America, all African,
523 Arabian and Central Asian semi-deserts, most of the southern half of Australia, and
524 north-eastern Siberia. The negative effect is also much more pronounced and
525 comprises most tropical savannahs (Fig. 8c-d). This creates opposing effects for the
526 large zone covering North Africa, Arabia and Central Asia, with climate change
527 leading to a decrease in plant productivity and fuel load (hence lower emissions)
528 against CO₂ change leading to CO₂ fertilisation (hence higher emissions).

529 For the moister and in general much more highly emitting savannahs (van der Werf et
530 al. 2010), the dominant effect comes from CO₂ change and is negative, due to shrub
531 encroachment. This creates an interesting situation for Australia: in the very north,
532 higher CO₂ leads to shrub encroachment, leading to lower emissions (Fig. 7); in a
533 central zone across the continent, climate change is the leading driver of increased

534 emissions, but for most of the southern half, CO₂ change leads to enhanced water-use
535 efficiency of the already woody vegetation (Morgan et al. 2007) causing the opposite
536 effect compared to the north. The same pattern is repeated for southern Africa, but
537 with a stronger positive climate effect in the central zone. The demographic effect
538 (Fig. 8e) leads to a significant increase in wildfire emissions in Central and Eastern
539 Europe as well as East Asia due to its projected declining population, but a decrease
540 mainly in African savannahs but also Turkey and Afghanistan/southern Central Asia
541 given their projected large increases in population.

542 **4 Discussion**

543 In this study, we find that wildfire emissions declined likely more than 10% during
544 the course of the 20th century, in agreement with ice core measurements of the
545 isotopic signature of carbon monoxide (Wang et al. 2010). A decline in global
546 wildfire activity since the late 19th century was also suggested by Marlon et al. (2008)
547 based on charcoal records, even though issues remain concerning the magnitude of
548 the decline as and whether there have also been periods of increasing emissions (van
549 der Werf et al., 2013). In the present simulations, the decline is caused
550 overwhelmingly by increasing population density, in agreement with the results of
551 Knorr et al. (2014) who used SIMFIRE alone to simulate burned area, without
552 coupling to LPJ-GUESS, driven by the same historical population data. According to
553 the present study, population effects dominated because a positive effect of climate
554 change on burned area was compensated by a negative effect on fuel load, and a
555 negative effect of CO₂ increase on burned area was compensated a positive effect on
556 fuel load. This broad general pattern, found for the main active wildfire regions, is
557 predicted to continue throughout the 21st century, albeit with much stronger climate

558 and CO₂ effects, while the negative population effect on emissions continues to have
559 about the same magnitude.

560 This dominant pattern of opposing climate and CO₂ effects, and opposing effects via
561 burned area and fuel load, calls for a mechanistic explanation. A positive impact of
562 climate change on burned area or numbers of fires is what is commonly expected
563 (Krawchuck et al. 2009, Pechony and Shindell 2010) and it was found for all regions
564 in agreement with simulated changes in fire risk (N_{max} in Eq. 1). The exception is the
565 Middle East region during the 20th century, with a negative climate impact on burned
566 area, which is likely caused by a decline in fuel continuity which suppresses the
567 spread of fires (reduced F in Eq. 1). A negative climate impact on fuel load is
568 consistent with the widely expected positive climate-carbon cycle feedback
569 (Friedlingstein et al. 2006), whereby rising temperatures increase soil and litter
570 respiration rates, releasing CO₂ from the terrestrial biosphere. The faster
571 decomposition of litter under warmer conditions, incorporated into LPJ-GUESS
572 (Smith et al. 2001), leads to a reduction in fuel available for combustion (Knorr et al.
573 2012). Since combustion by fire is nothing more than a shortcut for litter
574 decomposition, higher temperatures simply shift the balance between the two
575 processes towards microbial decomposition. However, the opposite climate effect
576 could also be expected, where warming leads to increased productivity in boreal,
577 temperature-limited ecosystems, leading to increased fuel production (Pausas and
578 Ribeiro 2013). For the present study, at least, this situation does not play a global role
579 and is only found for scattered regions of north-eastern Canada and northern Russia
580 (Fig. 6b).

581 A positive effect of CO₂ on fuel load, which is found to be active almost everywhere
582 across the globe, is fully consistent with the notion of CO₂ fertilisation of the

583 terrestrial biosphere (Long et al. 1996, Körner 2000), whereby higher atmospheric
584 CO₂ concentrations increase the rate of carboxylation, increasing net primary
585 production and thus fuel load (Hickler et al. 2008). However, we also find a negative
586 impact of rising CO₂ on wildfire emissions for all tropical savannah ecosystems,
587 which outweighs the positive impact through increasing fuel load and is caused by an
588 increase in the dominance of woody at the expense of grass vegetation. This
589 phenomenon of shrub encroachment, or woody thickening, in tropical savannahs has
590 been repeatedly observed in field studies (Wigley et al. 2010; Bond and Midgley
591 2012) and frequently attributed to CO₂ enrichment of the atmosphere (Morgan et al.
592 2007; Buitenwerf et al. 2012). This link is less observed for arid savannahs (Bond and
593 Midgley 2012), consistent with the finding here that in the most arid regions, no
594 decrease in the grass fraction is predicted.

595 On a global scale, according to the present simulations, the level of future wildfire
596 emissions is highly uncertain for a scenario of moderate greenhouse gas increases
597 (RCP4.5), with the ensemble mean showing slightly lower emissions towards the end
598 of the 21st as opposed to the end of the 20th century. For a high, business-as-usual
599 scenario of greenhouse gas forcing (RCP8.5), the ensemble mean points towards an
600 increase across the same time span, but with a range including both positive and
601 negative changes. There is also a general trend towards increases during the second
602 half of this century. The slight bias towards increased emissions is the result of a
603 combination of increased fire risk due to warming, and increased fuel load due to CO₂
604 fertilisation, but with population growth, woody thickening and faster litter
605 decomposition all counteracting. We therefore find that climatic impacts on fire risk
606 are only one of many, often opposing factors that might lead to increased wildfire
607 emissions in the future.

608 The future demographic dynamics can lead to a wide range of future wildfire
609 emissions. In addition to its indirect impact on wildfire emissions through interactions
610 with economic and technological changes contributing to GHGs emissions and
611 climate change, changes in population size and spatial distribution play a direct and
612 important role for fire prevalence, as an ignition source but predominantly as fire
613 suppressors. While fertility decline is occurring in almost all global regions, the
614 population momentum will continue to drive global population size upward for at
615 least some years and likely contribute to continuously declining wildfire frequencies.
616 The uncertainty of future population dynamics, however, leads to a wide range of
617 population trends and causes large variations in simulated wildfire emissions.
618 Moreover, the same changes in population sizes can result in rather different
619 emissions due to variations in spatial population distribution, particularly through
620 different urbanisation patterns. While the whole world is expected to be further
621 urbanised, variations in speed and patterns of urbanisation across regions and over
622 time can lead to significantly different wildfire patterns.

623 Simulated emissions presented here generally agree with similar results with a
624 coupled fire-vegetation-biogeochemical model by Kloster et al. (2012), insofar as
625 climate only starts to impact on fire during the course of the 21st century, but not
626 before, and that changes in population density generally lead to lower emissions. The
627 difference is that in the present study, climate has a much smaller impact on
628 emissions, ranging between 0 and +20% for RCP8.5 and few percent at most for
629 RCP4.5. A similar study reporting simulations of increasing fire emissions for Europe
630 (Migliavacca et al. 2013a) reports an increase for Europe of about 15 TgC yr⁻¹ until
631 the late 21st century, when measured for the same reference period as here, which is
632 within the ensemble range found in this study. Even though they used the same

633 Community Land Model, their fire parameterisation (Migliavacca et al. 2013b)
634 differed from the one used by Kloster et al. (2012). Our results also differ partly from
635 those by Lasslop and Kloster (2015), who simulated increased combustible fuel load
636 (emission per burned area) during the 20th century, but in their case woody thickening
637 did not counteract the increase by reducing burned area. As a result, emissions
638 increased by approximately 40% over that period, with about half of the increase due
639 to increasing burned area.

640 The difference between the present study and the one by Kloster et al. (2012) and
641 Lasslop and Kloster (2015) might be due to the pronounced negative effect of
642 temperature change on fuel load, and of CO₂ on burned area, found here. Another
643 important difference is that their study included deforestation fires, and employed the
644 more common approach of representing the impact of population density by a
645 combination of number of ignitions times an explicit function of fire suppression, the
646 combination of which leads to a small decrease in emissions during the 21st century.
647 This approach, based on Venevsky et al. (2002), always leads to an increase in burned
648 area if ignitions increase, all else being equal. Kloster et al. (2012) simulate no decline
649 during the 20th century, neither due to changing population density, nor land use. This
650 study, by contrast, uses a semi-empirical approach with a functional form of the
651 relationship between burned area and population density derived by optimisation
652 against observed burned area and simulates the historical decline that is suggested on
653 the basis of ice core and charcoal records. The implicit assumption here is that that for
654 most of the world, except for areas where population density is very low, the fire
655 regime is ignition saturated (Guyette et al. 2002), in contradiction to the approach by
656 Venevsky et al. (2002). This means that above a threshold of typically 0.1 inhabitants
657 per km², burned area becomes independent of human population density (cf. Knorr et

658 al. 2014). However, if we assume some increase in burned area with population
659 density below the threshold, the results change only little (Fig. 3). Therefore we argue
660 for universal ignition saturation as a reasonable approximation at the scales
661 considered in the present study. We also expect possible future increases in lightning
662 activity (Romps et al. 2014) to have only a marginal effect on burned area and thus
663 emissions.

664 An important outcome of this study is that it predicts a large shift in fire emissions
665 from the tropics towards the extra-tropics, driven by two coinciding effects causing a
666 secular decline in emissions in African savannahs and grasslands: CO₂ increases
667 driving woody thickening, in turn making the vegetation less flammable (Bond and
668 Midgley 2012), and population growth leading to decreased burned area (Archibald et
669 al. 2008). The impact of this shift on the global budget of carbon emissions from
670 wildfires is so large because these regions currently have by far the largest emissions
671 worldwide (van der Werf et al. 2010). In agreement with observed evidence (Bond
672 and Midgley 2012), the negative CO₂ effect on emissions via burned area is limited to
673 the semi-humid tropics and does not play a role either in the most arid regions, nor at
674 higher latitudes. It is also not simulated for South Asia, where most of the potential
675 semi-humid grasslands and savannahs have long been converted to agriculture. For
676 the mostly arid region Middle East, we find that a strong positive CO₂ effect via
677 burned area is the larger contributor to emission change during the 20th century, and
678 the biggest during the 21st. This leads to a marked increase in emissions for RCP8.5,
679 outcompeting negative impacts of growing population and climate change on fuel
680 load and driven by a marked decline in precipitation (Table 1), while during the 20th
681 century, there is a marked negative impact of climate change on burned area. Here,
682 CO₂ fertilisation leads to denser vegetation, increasing fuel continuity (higher F in Eq.

683 1), thus leading to higher burned area, while decreasing precipitation results in a
684 lower F . To a lesser extent this is simulated for North Asia, which also contains large,
685 highly arid regions, but with a positive ensemble-mean climate effect on burned area.
686 For both regions, however, the ensemble spread is very large making the projections
687 highly uncertain.

688 For Australia, we find an interesting zonal pattern of changing effects from the
689 northern savannahs to the arid southern coast. In the very north, woody thickening
690 due to higher CO_2 leads to decreased emissions through decreased burned area, with
691 negligible climate effects. This is followed by a central zone where both climate and
692 CO_2 change lead to increased emissions, and a third zone comprising the southern half
693 of the Australian interior where CO_2 fertilisation leads to increased emissions via
694 higher productivity. Population change plays almost no role for changing emissions in
695 this region. As a result, the north is predicted to decrease significantly in emissions,
696 while for the central zone where climate and CO_2 effects overlap, and for the south
697 there is no clear signal in the prediction. A similar tri-zonal pattern is also predicted
698 for southern Africa stretching from the Miombo woodlands across the Kalahari to the
699 Cape region. This zonal differentiation resembles the results by Kelley and Harrison
700 (2014), who simulated a reduction in burned area in North Australia due to CO_2
701 driven woody thickening, but an increase in burned area in the Australian interior due
702 to enhanced fuel continuity with denser vegetation caused by CO_2 fertilisation.

703 **5 Conclusions**

704 We find that since the early 20th century, wildfire emissions have been steadily
705 declining due to expanding human population, but that this decline will only continue
706 if climate change and atmospheric CO_2 rise is limited to low or low/moderate levels,
707 population continues to grow and urbanisation follows a slow pathway in the next

708 decades. Otherwise, it is likely that the world is currently in a historic minimum
709 regarding wildfire emissions, and the current declining emission trend will reverse in
710 the future at higher latitudes, departing from the current domination of African
711 savannahs. Emissions, however, are unlikely until 2100 to again reach early 20th
712 century levels. The predictions are based on an ensemble of climate and
713 population/urbanisation projections, but a single fire model albeit tested for the impact
714 of different parameterisations. The results generally show a large ensemble spread,
715 and also reveal widely opposing factors influencing future emissions, complicating
716 the task of predicting future wildfire emissions. We find that apart from climate
717 leading to higher fire risk, equally important factors on a global scale are demographic
718 change, woody thickening in savannahs with higher CO₂ levels, and faster woody or
719 grass litter turnover in a warmer climate, both leading to declining emission, as well
720 as CO₂ fertilisation generally leading to higher fuel loads or fuel continuity and thus
721 increased emissions. Therefore, the common view of climate warming as the
722 dominant driver of higher future wildfire emissions cannot be supported.

723 This work is assumes that fire management for a given fire and vegetation regime
724 will remain unchanged. New fire policies that go beyond simple fire suppression
725 and thus avoid large-scale fuel build-up and ultimately increased risks of large
726 fires could very well counteract the effects of climate change and thus lead to
727 a better co-existence between humans, natural ecosystems and wildfires.

728 **Author contribution**

729 W. K. conceived the study, processed the input data, carried out model runs,
730 performed the analysis and wrote the first full draft of the manuscript, L. J. provided
731 the population scenarios, all authors contributed to discussions of results and writing.

732 **Acknowledgements**

733 This work was supported by EU contracts 265148 (Pan-European Gas-Aerosol-
734 climate interaction Study, PEGASOS) and grant 603542 (Land-use change: assessing
735 the net climate forcing, and options for climate change mitigation and adaptation,
736 LUC4C). We thank Thomas Hickler for pointing out relevant literature on woody
737 thickening.

738 **References**

- 739 Ahlström, A., Schurgers, G., Arneth, A., and Smith, B.: Robustness and uncertainty in
740 terrestrial ecosystem carbon response to CMIP5 climate change projections, *Env.*
741 *Res. Lett.*, 7, 044008, doi:10.1088/1748-9326/7/4/044008, 2012.
- 742 Andela, N. and van der Werf, G. R.: Recent trends in African fires driven by cropland
743 expansion and El Nino to La Nina transition, *Nature Climate Change*, 4, 791-795,
744 2014.
- 745 Archibald, S., Roy, D. P., van Wilgen, B. W., and Scholes, R. J.: What limits fire? An
746 examination of drivers of burnt area in Southern Africa, *Global Change Biol*, 15,
747 613-630, 2008.
- 748 Arneth, A., Harrison, S. P., Zaehle, S., Tsigaridis, K., Menon, S., Bartlein, P. J.,
749 Feichter, J., Korhola, A., Kulmala, M., O'Donnell, D., Schurgers, G., Sorvari, S.,
750 and Vesala, T.: Terrestrial biogeochemical feedbacks in the climate system, *Nat*
751 *Geosci*, 3, 525-532, 2010.
- 752 Bistinas, I., Harrison, D. E., Prentice, I. C., and Pereira, J. M. C.: Causal relationships
753 vs. emergent patterns in the global controls of fire frequency, *Biogeosci.*, 11,
754 5087–5101, doi:10.5194/bg-11-5087-2014, 2014.
- 755 Bond, W. J. and Midgley, G. F.: Carbon dioxide and the uneasy interactions of trees
756 and savannah grasses, *Phil. Trans. R. Soc. B*, 367, 601-612, 2012.

757 Bowman, D. M. J. S., Balch, J. K., Artaxo, P., Bond, W. J., Carlson, J. M., Cochrane,
758 M. A., D'Antonio, C. M., DeFries, R. S., Doyle, J. C., Harrison, S. P., Johnston, F.
759 H., Keeley, J. E., Krawchuk, M. A., Kull, C. A., Marston, J. B., Moritz, M. A.,
760 Prentice, I. C., Roos, C. I., Scott, A. C., Swetnam, T. W., van der Werf, G. R., and
761 Pyne, S. J.: Fire in the Earth System, *Science*, 324, 481-484, 2009.

762 Buitenwerf, R., Bond, W. J., Stevens, N., and Trollope, W. S. W.: Increased tree
763 densities in South African savannas: > 50 years of data suggests CO₂ as a driver,
764 *Global Change Biol*, 18, 675-684, 2012.

765 Claussen, M., Brovkin, V., and Ganopolski, A.: Biogeophysical versus
766 biogeochemical feedbacks of large-scale land cover change, *Geophys. Res. Let.*,
767 28, 1011-1014, 2001.

768 Friedlingstein, P., Cox, P. M., Betts, R. A., Bopp, L., von Bloh, W., Brovkin, V.,
769 Cadule, P., Doney, S., Eby, M., Fung, I., Bala, G., John, J., Jones, C. D., Joos, F.,
770 Kato, T., Kawamiya, M., Knorr, W., Lindsay, K., Matthews, H. D., Raddatz, T.,
771 Rayner, P. J., Reick, C., Roeckner, E., Schnitzler, K.-G., Schnur, R., Strassmann,
772 K., Weaver, A. J., Yoshikawa, C., and Zeng, N.: Climate-carbon cycle feedback
773 analysis, results from the C4MIP model intercomparison, *J. Climate*, 19, 3337-
774 3353, 2006.

775 Giglio, L., Randerson, J. T., van der Werf, G. R., Kasibhatla, P. S., Collatz, G. J.,
776 Morton, D. C., and DeFries, R. S.: Assessing variability and long-term trends in
777 burned area by merging multiple satellite fire products *Biogeosci.*, 7, 1171-1186,
778 2010.

779 Giglio, L., Randerson, J. T., and van der Werf, G. R.: Analysis of daily, monthly, and
780 annual burned area using the fourth-generation global fire emissions database
781 (GFED4), *J Geophys Res-Bioge*, 118, 317-328, 2013.

782 Guyette, R. P., Muzika, R. M., and Dey, D. C.: Dynamics of an anthropogenic fire
783 regime, *Ecosystems*, 5, 472-486, 2002.

784 Harris, I., Jones, P. D., Osborn, T. J., and Lister, D. H.: Updated high-resolution grids
785 of monthly climatic observations – the CRU TS3.10 Dataset, *Int. J. Climatol.*, 34,
786 623-642, 2014.

787 Hickler, T., Smith, B., Prentice, I. C., Mjöfors, K., Miller, P., Arneth, A., and Sykes,
788 M. T.: CO₂ fertilization in temperate FACE experiments not representative of
789 boreal and tropical forests, *Global Change Biol*, 14, 1531-1542, 2008.

790 Hurtt, G. C., Chini, L. P., Frohking, S., Betts, R. A., Feddema, J., Fischer, G., Fisk, J.
791 P., Hibbard, K., Houghton, R. A., Janetos, A., Jones, C. D., Kindermann, G.,
792 Kinoshita, T., Goldewijk, K. K., Riahi, K., Shevliakova, E., Smith, S., Stehfest, E.,
793 Thomson, A., Thornton, P., van Vuuren, D. P., and Wang, Y. P.: Harmonization of
794 land-use scenarios for the period 1500-2100: 600 years of global gridded annual
795 land-use transitions, wood harvest, and resulting secondary lands, *Climatic*
796 *Change*, 109, 117-161, 2011.

797 Jiang, L.: Internal consistency of demographic assumptions in the shared
798 socioeconomic pathways, *Popul. Environ.*, 35, 261-285, 2014.

799 Kasischke, E. S. and Penner, J. E.: Improving global estimates of atmospheric
800 emissions from biomass burning, *J. Geophys. Res.*, 109, D14S01,
801 doi:10.1029/2004JD004972, 2004.

802 Kelley, D. I. and Harrison, S. P.: Enhanced Australian carbon sink despite increased
803 wildfire during the 21st century, *Environ. Res. Lett.*, 9, 104015, doi: 10.1088/1748-
804 9326/9/10/104015, 2014.

805 Klein Goldewijk, K., Beusen, A., and Janssen, P.: Long-term dynamic modeling of
806 global population and built-up area in a spatially explicit way: HYDE 3.1,
807 *Holocene*, 20, 565-573, 2010.

808 Kloster, S., Mahowald, N. M., Randerson, J. T., and Lawrence, P. J.: The impacts of
809 climate, land use, and demography on fires during the 21st century simulated by
810 CLM-CN, *Biogeosciences*, 9, 509-525, 2012.

811 Knorr, W., Lehsten, V., and Arneth, A.: Determinants and predictability of global
812 wildfire emissions, *Atm. Chem. Phys.*, 12, 6845–6861, 2012.

813 Knorr, W., Kaminski, T., Arneth, A., and Weber, U.: Impact of human population
814 density on fire frequency at the global scale, *Biogeosci.*, 11, 1085-1102, 2014.

815 Körner, C.: Biosphere responses to CO₂ enrichment, *Ecological Applications*, 10,
816 1590-1619, 2000.

817 Krawchuk, M. A., Moritz, M. A., Parisien, M. A., Van Dorn, J., and Hayhoe, K.:
818 Global Pyrogeography: the Current and Future Distribution of Wildfire, *Plos One*,
819 4, e5102, doi:10.1371/journal.pone.0005102, 2009.

820 Langmann, B., Duncan, B., Textor, C., Trentmann, J., and van der Werf, G. R.:
821 Vegetation fire emissions and their impact on air pollution and climate, *Atmos*
822 *Environ*, 43, 107-116, 2009.

823 Long, S. P., Osborne, C. P., and Humphries, S. W.: Photosynthesis, rising
824 atmospheric carbon dioxide concentration and climate change. In: *Global change:*
825 *Effects on coniferous forests and grasslands*, Breymeyer, A. I., Hall, D. O.,
826 Melillo, J. M., and Ågren, G. I. (Eds.), Scope, Wiley & Sons, New York, 1996.

827 Marlon, J. R., Bartlein, P. J., Carcaillet, C., Gavin, D. G., Harrison, S. P., Higuera, P.
828 E., Joos, F., Power, M. J., and Prentice, I. C.: Climate and human influences on

829 global biomass burning over the past two millennia, *Nature Geosci.*, 1, 697-702,
830 2008.

831 Martin Calvo, M. and Prentice, I. C.: Effects of fire and CO₂ on biogeography and
832 primary production in glacial and modern climates, *New Phytologist*, 208, 987-
833 994, 2015.

834 Meinshausen, M., Smith, S. J., Calvin, K., Daniel, J. S., Kainuma, M. L. T.,
835 Lamarque, J.-F., Matsumoto, K., Montzka, S. A., Raper, S. C. B., Riahi, K.,
836 Thomson, A., Velders, G. J. M., and van Vuuren, D. P. P.: The RCP greenhouse
837 gas concentrations and their extensions from 1765 to 2300, *Climatic Change*, 109,
838 213-241, 2011.

839 Migliavacca, M., Dosio, A., Camia, A., Houbourg, R., Houston Durtant, T., Kaiser, J.
840 W., Khabarov, N., Krasovskii, A. A., Marcolla, B., Miguel-Ayanz, J., Ward, D. S.,
841 and Cescatti, A.: Modeling biomass burning and related carbon emissions during
842 the 21st century in Europe, *J. Geophys. Res.*, 118, 1732–1747, 2013a.

843 Migliavacca, M., Dosio, A., Kloster, S., Ward, D. S., Camia, A., Houborg, R.,
844 Houston Durtant, T., Khabarov, N., Krasovskii, A. A., San Miguel-Ayanz, J., and
845 Cescatti, A.: Modeling burned area in Europe with the Community Land Model, *J*
846 *Geophys Res*, 118, 265–279, 2013b.

847 Morgan, J. A., Milchunas, D. G., LeCain, D. R., West, M., and Mosier, A. R.: Carbon
848 dioxide enrichment alters plant community structure and accelerates shrub growth
849 in the shortgrass steppe, *Proc. Nat. Acad. Sci. USA*, 104, 14724-14729, 2007.

850 Moritz, M. A., Parisien, M.-A., Batllori, E., Krawchuk, M. A., Van Dorn, J., Ganz, D.
851 J., and Hayhoe, K.: Climate change and disruptions to global fire activity,
852 *Ecosphere*, 3, 49, doi:10.1890/ES11-00345.1, 2012.

853 O'Neill, B., Carter, T. R., Ebi, K. L., Edmonds, J., Hallegatte, S., Kemp-Benedict, E.,
854 Kriegler, E., Mearns, L., Moss, R., Riahi, K., van Ruijven, B., and van Vuuren, D.:
855 Workshop on The Nature and Use of New Socioeconomic Pathways for Climate
856 Change Research, Boulder, CO, November 2–4 2011, available at:
857 [https://www2.cgd.ucar.edu/sites/default/files/iconics/Boulder-Workshop-](https://www2.cgd.ucar.edu/sites/default/files/iconics/Boulder-Workshop-Report.pdf)
858 [Report.pdf](https://www2.cgd.ucar.edu/sites/default/files/iconics/Boulder-Workshop-Report.pdf) (last access: 9 September 2015, National Center for Atmospheric
859 Research (NCAR), Boulder, CO, 2012.

860 Pechony, O. and Shindell, D. T.: Driving forces of global wildfires over the past
861 millennium and the forthcoming century, *Proc. Natl. Acad. Sci. USA*, 107, 19167-
862 19170, 2010.

863 Pausas, J. G. and Ribeiro, E.: The global fire–productivity relationship, *Global Ecol*
864 *Biogeogr*, 22, 728-736, 2013.

865 Ramankutty, N. and Foley, J. A.: Estimating historical changes in global land cover:
866 Croplands from 1700 to 1992, *Global Biogeochemical Cycles*, 13, 997-1027, 1999.

867 Randerson, J., Chen, Y., van der Werf, G. R., Rogers, B. M., and Morton, D. C.:
868 Global burned area and biomass burning emissions from small fires, *J. Geophys.*
869 *Res.*, 117, G04012, doi:10.1029/2012JG002128, 2012.

870 Romps, D. M., Seeley, J. T., Vollaro, D., and Molinari, J.: Projected increase in
871 lightning strikes in the United States due to global warming, *Science*, 346, 851-
872 854, 2014.

873 Roy, D. P., Boschetti, L., Justice, C. O., and Ju, J.: The collection 5 MODIS burned
874 area product - Global evaluation by comparison with the MODIS active fire
875 product, *Remote Sens Environ*, 112, 3690-3707, 2008.

876 Scholze, M., Knorr, W., Arnell, N. W., and Prentice, I. C.: A climate-change risk
877 analysis for world ecosystems, *Proc. Nat. Acad. Sci. USA*, 103, 13116-13120,
878 2006.

879 Smith, B., Prentice, C., and Sykes, M.: Representation of vegetation dynamics in
880 modelling of terrestrial ecosystems: comparing two contrasting approaches within
881 European climate space, *Global Ecol Biogeogr*, 10, 621-637, 2001.

882 Stein, U. and Alpert, P.: Factor separation in numerical simulations, *Journal of the*
883 *Atmospheric Sciences*, 50, 2107-2115, 1993.

884 Taylor, K. E., Stouffer, R. J., and Meehl, G. A.: An overview of CMIP5 and the
885 experiment design, *Bull. Am. Meteorol. Soc.*, 93, 485-498, 2012.

886 Thonicke, K., Spessa, A., Prentice, I. C., Harrison, S. P., Dong, L., and Carmona-
887 Moreno, C.: The influence of vegetation, fire spread and fire behaviour on biomass
888 burning and trace gas emissions: results from a process-based model,
889 *Biogeosciences*, 7, 1991-2011, 2010.

890 van der Werf, G. R., Randerson, J. T., Giglio, L., Collatz, G. J., Mu, M., Kasibhatla,
891 P. S., Morton, D. C., Defries, R. S., Jin, Y., and van Leeuwen, T. T.: Global fire
892 emissions and the contribution of deforestation, savanna, forest, agricultural, and
893 peat fires (1997-2009), *Atmos. Chem. Phys.*, 10, 11707-11735, 2010.

894 van der Werf, G. R., Peters, W., van Leeuwen, T. T., and Giglio, L.: What could have
895 caused pre-industrial biomass burning emissions to exceed current rates?, *Clim.*
896 *Past*, 9, 289-306, 2013.

897 van Vuuren, A. J., Edmonds, J., Kainuma, M., Riahi, K., Thomson, A., Hibbard, K.,
898 Hurtt, G. C., Kram, T., Krey, V., Lamarque, J. F., Masui, T., Meinshausen, M.,
899 Naicenovic, N., Smith, S. J., and Rose, S. K.: The representative concentration
900 pathways: an overview, *Clim. Change*, 109, 5-31, 2011.

901 Venevsky, S., Thonicke, K., Sitch, S., and Cramer, W.: Simulating fire regimes in
902 human-dominated ecosystems: Iberian Peninsula case study, *Global Change*
903 *Biology*, 8, 984-998, 2002.

904 Wang, Z., Chappellaz, J., Park, K., and Mak, J. E.: Large variations in Southern
905 Hemisphere biomass burning during the last 650 years, *Science*, 330, 1663-1666,
906 2010.

907 Wigley, B. J., Bond, W. J., and Hoffman, M. T.: Thicket expansion in a South African
908 savanna under divergent land use: local vs. global drivers?, *Global Change Biol*,
909 16, 964-976, 2010.

910 **Tables**

911 *Table 1: Simulated changes in climate by region*.*

Absolute change in annual-mean temperature [K]*									
Region	historical ⁽¹⁾			RCP4.5 ⁽²⁾			RCP8.5 ⁽²⁾		
North America	0.62	(0.03,	1.18)	3.15	(1.88,	4.90)	5.70	(3.78,	7.97)
Europe	0.50	(-0.20,	1.00)	2.56	(1.77,	3.83)	4.53	(3.46,	6.26)
North Asia	0.51	(0.07,	0.98)	3.25	(2.13,	4.81)	5.69	(3.91,	7.63)
Middle East	0.50	(0.09,	0.86)	2.71	(1.82,	3.78)	5.05	(3.68,	6.33)
South America	0.43	(0.07,	0.78)	2.36	(1.65,	3.19)	4.34	(2.83,	5.39)
Africa	0.47	(0.08,	0.72)	2.54	(1.77,	3.34)	4.67	(3.48,	5.87)
South Asia	0.37	(0.01,	0.65)	2.28	(1.60,	3.06)	4.07	(2.95,	5.09)
Oceania	0.44	(0.17,	0.74)	2.18	(1.35,	2.83)	4.16	(2.83,	5.35)
Globe	0.50	(0.08,	0.83)	2.77	(1.83,	3.89)	5.01	(3.49,	6.48)
Relative change in mean annual precipitation*									
North America	-0.5%	(-1.8%,	1.6%)	4.6%	(-2.1%,	7.6%)	5.3%	(-5.7%,	10.8%)
Europe	-1.0%	(-4.5%,	1.5%)	1.9%	(-3.0%,	10.7%)	0.6%	(-5.6%,	13.1%)
North Asia	-0.8%	(-3.3%,	1.0%)	9.4%	(5.8%,	15.1%)	13.8%	(8.2%,	19.7%)
Middle East	-6.4%	(-11.8%,	0.9%)	-6.0%	(-17.0%,	5.7%)	-10.7%	(-28.3%,	0.0%)
South America	-2.5%	(-6.8%,	-0.9%)	-0.7%	(-8.8%,	11.7%)	-1.3%	(-10.6%,	14.3%)
Africa	-2.7%	(-9.3%,	0.1%)	1.4%	(-6.3%,	5.0%)	2.7%	(-5.0%,	9.6%)
South Asia	-1.2%	(-6.0%,	1.8%)	8.3%	(4.9%,	12.8%)	14.5%	(9.0%,	22.3%)
Oceania	-1.5%	(-7.2%,	2.7%)	-1.9%	(-27.2%,	6.6%)	-6.7%	(-38.3%,	11.8%)
Globe	-1.8%	(-3.2%,	0.1%)	3.3%	(-1.1%,	5.6%)	4.7%	(0.8%,	7.6%)

* Mean across 8-ESM ensemble, ensemble minimum and maximum in parentheses.

⁽¹⁾ Changes from 1901-1930 to 1971-2000.

⁽²⁾ Changes from 1971-2000 to 2071-2100.

912 Table 2: Temporal average of global wildfire emissions in TgC/yr by time period, scenario and ESM*.

Period	RCP	Population growth	Urbanisation	ESM Ensemble	MPI-ESM-LR ⁽¹⁾	CCSM4 ⁽²⁾	CSIRO-Mk3.6 ⁽³⁾	EC-EARTH ⁽⁴⁾	CNRM-CM5 ⁽⁵⁾	GISS-E2-R ⁽⁶⁾	IPSL-CM5A-MR ⁽⁷⁾	HADGEM2-ES ⁽⁸⁾
1901-1930	-	Historical	Historical	1.43	1.44	1.42	1.46	1.42	1.43	1.42	1.44	1.39
1971-2000				<i>1.28</i>	<i>1.32</i>	<i>1.27</i>	<i>1.28</i>	<i>1.29</i>	<i>1.29</i>	<i>1.25</i>	<i>1.28</i>	<i>1.27</i>
2071-2100	4.5	low	fast	1.31	1.36	1.31	1.27	1.31	1.29	1.27	1.33	1.36
		intermediate	fast	1.27	1.32	1.27	1.23	1.26	1.26	1.23	1.29	1.32
		intermediate	central	1.22	1.26	1.22	1.17	1.20	1.20	1.18	1.23	1.27
		intermediate	slow	1.17	1.21	1.16	1.13	1.15	1.15	1.13	1.18	1.21
		high	slow	1.11	1.15	1.11	1.07	1.09	1.09	1.07	1.12	1.16
	8.5	low	fast	1.43	1.52	1.45	1.41	1.38	1.41	1.37	1.42	1.50
		intermediate	fast	1.39	1.47	1.41	1.38	1.34	1.36	1.33	1.38	1.46
		intermediate	central	1.33	1.41	1.36	1.32	1.29	1.30	1.28	1.33	1.40
		intermediate	slow	1.28	1.35	1.31	1.26	1.24	1.25	1.23	1.27	1.35
		high	slow	1.22	1.29	1.24	1.19	1.18	1.19	1.18	1.22	1.28

¹⁾ Max Planck Institute for Meteorology; ²⁾ National Centre for Atmospheric Research

³⁾ Commonwealth Scientific and Industrial Research Organisation in collaboration with Queensland CSIRO Climate Change Centre of Excellence

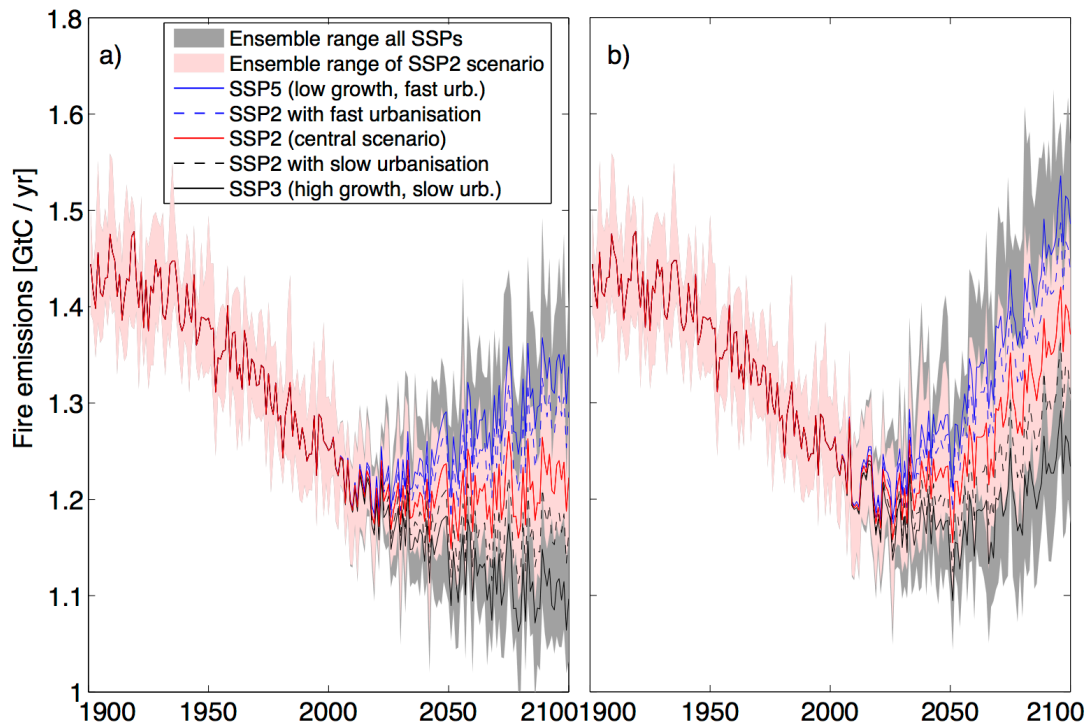
⁴⁾ EC-EARTH consortium

⁵⁾ Centre National de Recherches Météorologiques / Centre Européen de Recherche et Formation Avancée en Calcul Scientifique

⁶⁾ NASA Goddard Institute for Space Studies; ⁷⁾ Institut Pierre-Simon Laplace; ⁸⁾ Met Office Hadley Centre

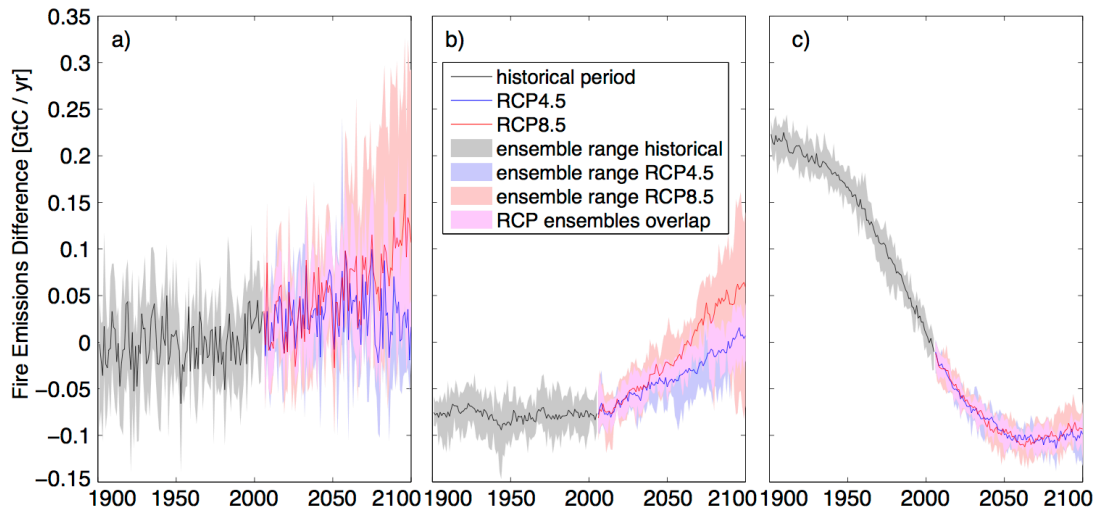
* Emissions larger than during 1971-2000 (italics) are shown in bold.

909 **Figures**



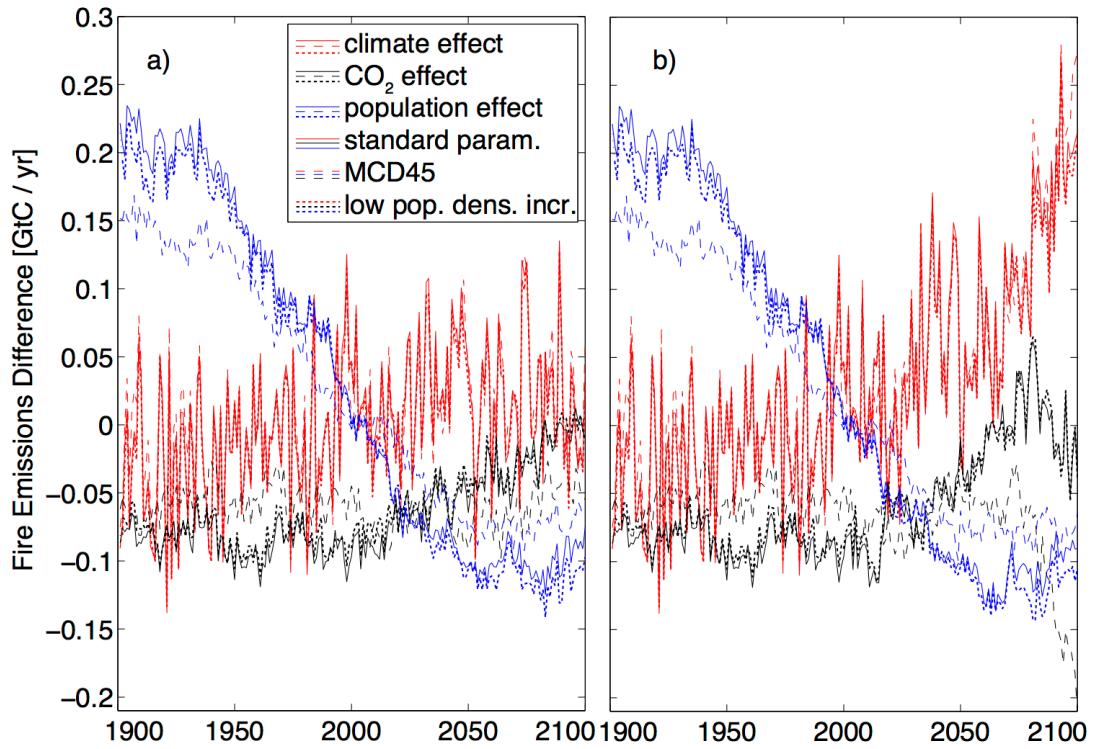
910
911 *Figure 1: Simulated global wildfire emissions 1900 to 2100. Shaded areas are for the*
912 *range of ensemble members either across all ESMs using only the central population*
913 *scenario SSP2, or across ESMs and all population scenarios. Lines show ensemble*
914 *averages for specific population scenarios. a) RCP4.5 greenhouse gas concentrations*
915 *and climate change; b) RCP8.5.*

916



917

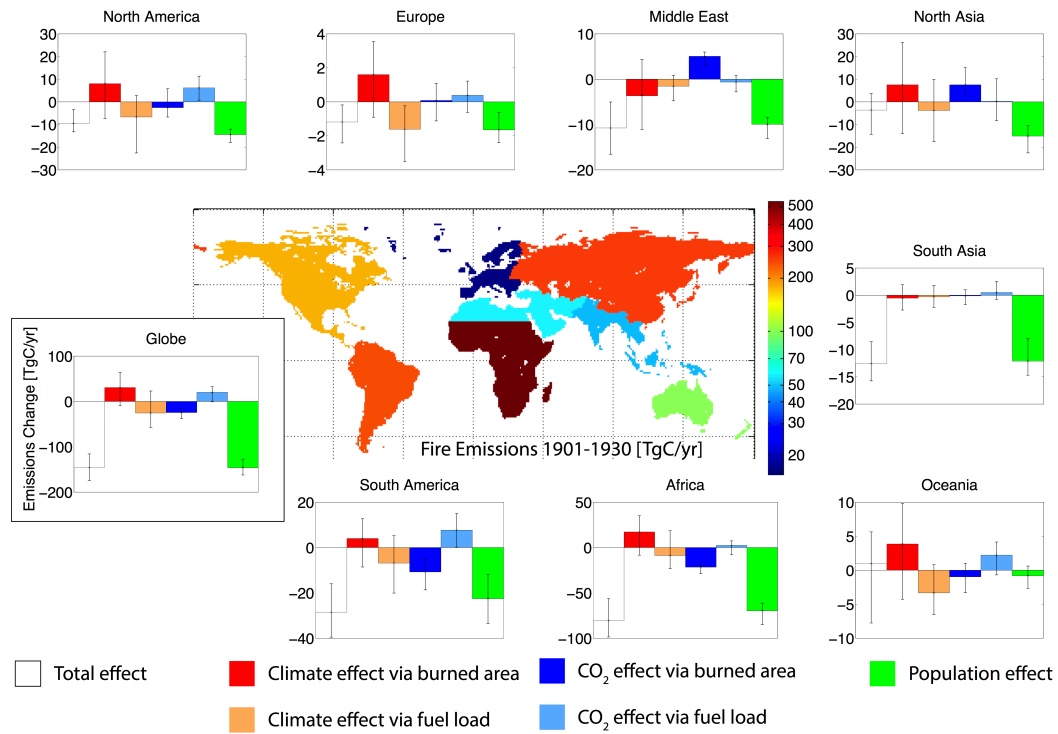
918 *Figure 2: Effects of different factors on global emissions for historical change (until*
 919 *2005) and two future climate change scenarios (RCP4.5 and RCP8.5). a) Effect of*
 920 *climate change, b) effect of changing atmospheric CO₂, c) effect of changing human*
 921 *population density. All simulations are for the central SSP2 population scenario.*
 922 *Solid lines for ESM ensemble means and shaded areas for the range across eight*
 923 *ESM simulations each.*



924

925 *Figure 3: Impact of changing fire model parameterisation on the simulated climate,*
 926 *CO₂ and population effects on emissions. Standard parameterisation of SIMFIRE*
 927 *optimised against GFED3 burned area, optimisation against MCD45 burned area,*
 928 *and simulation assuming an increasing effect of population density on burned area*
 929 *between 0 and 0.1 inhabitants / km². a) RCP4.5. b) RCP8.5.*

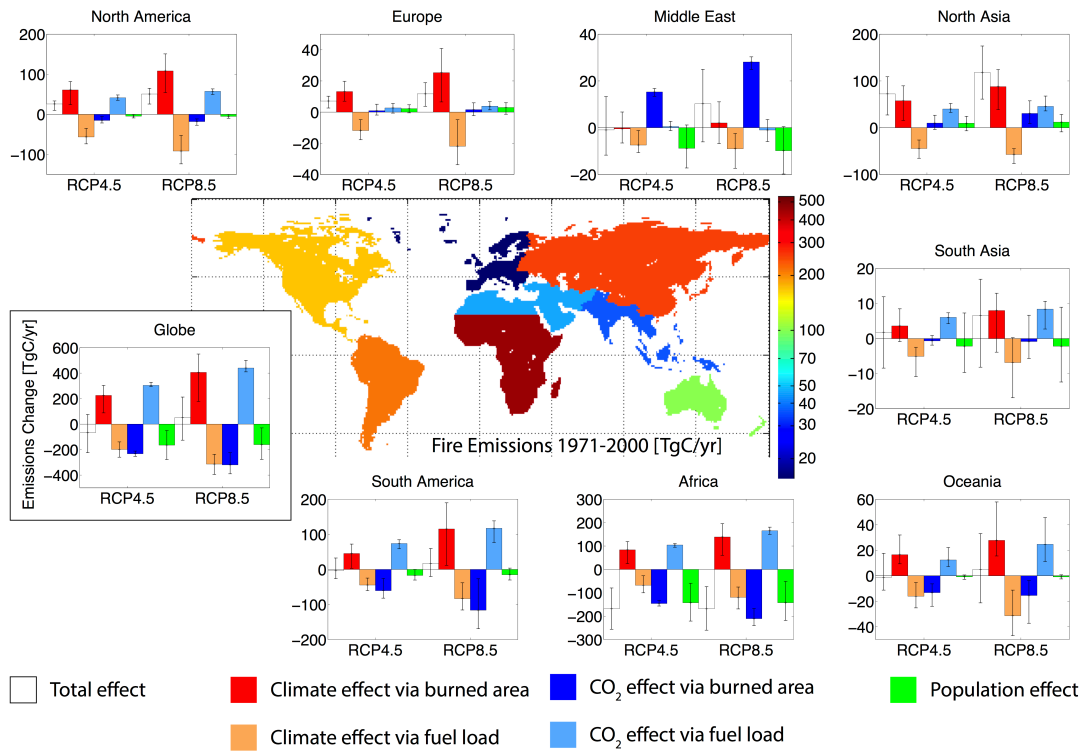
930



931

932 *Figure 4: Regional wildfire emissions during 1901-1930 for eight regions and global*
 933 *and regional changes, average 1971-2000 minus average 1901-1930, for ensemble*
 934 *mean (white/coloured bars) and range across ensemble comprising eight ESMs (error*
 935 *bars), in TgC/yr. The change in emissions is further subdivided into climate effect due*
 936 *to changes in burned area or changes in combusted fuel per burned area, effect of*
 937 *atmospheric CO₂ change due to changed burned are or fuel combustion, and*
 938 *population effect.*

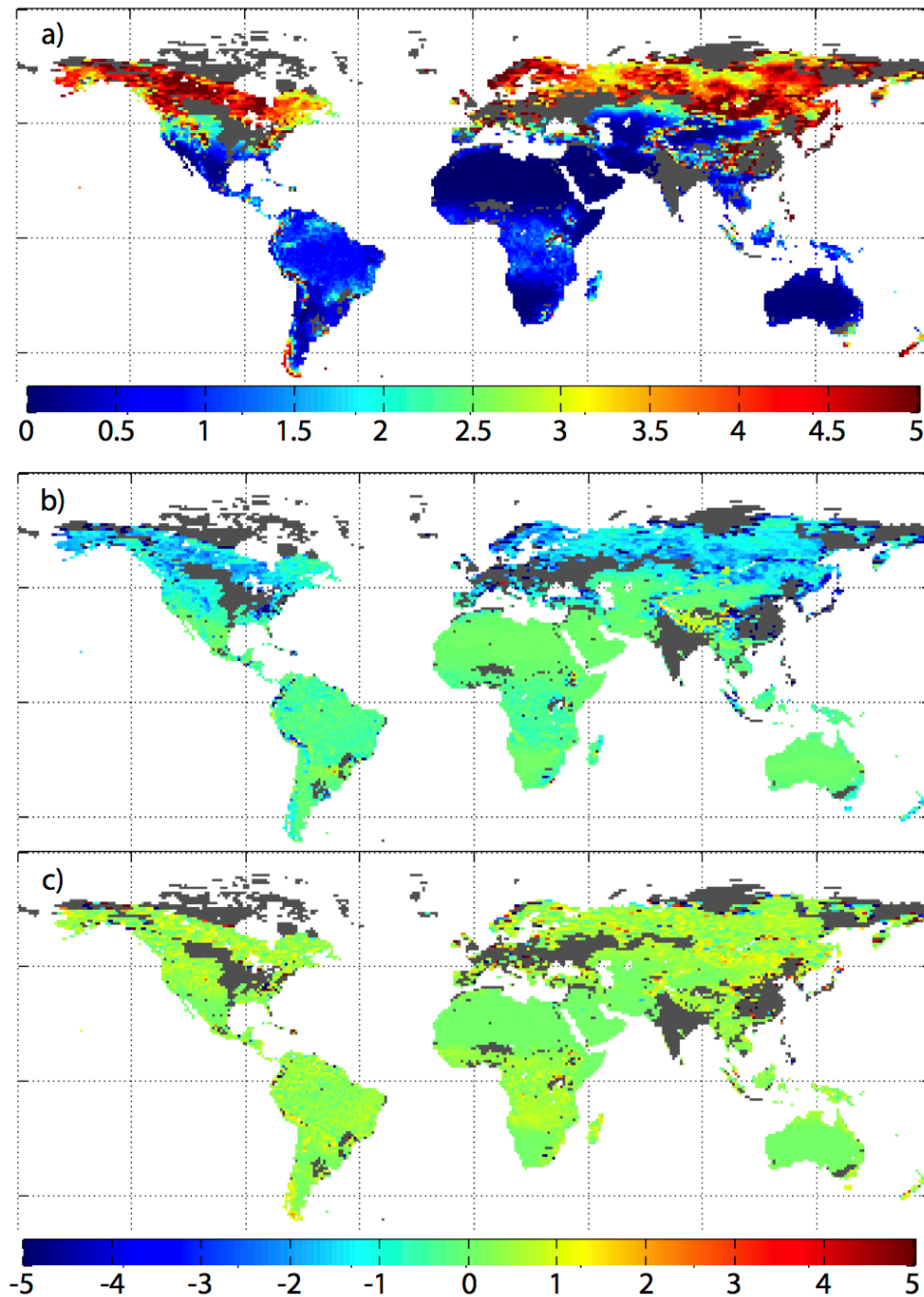
939



940

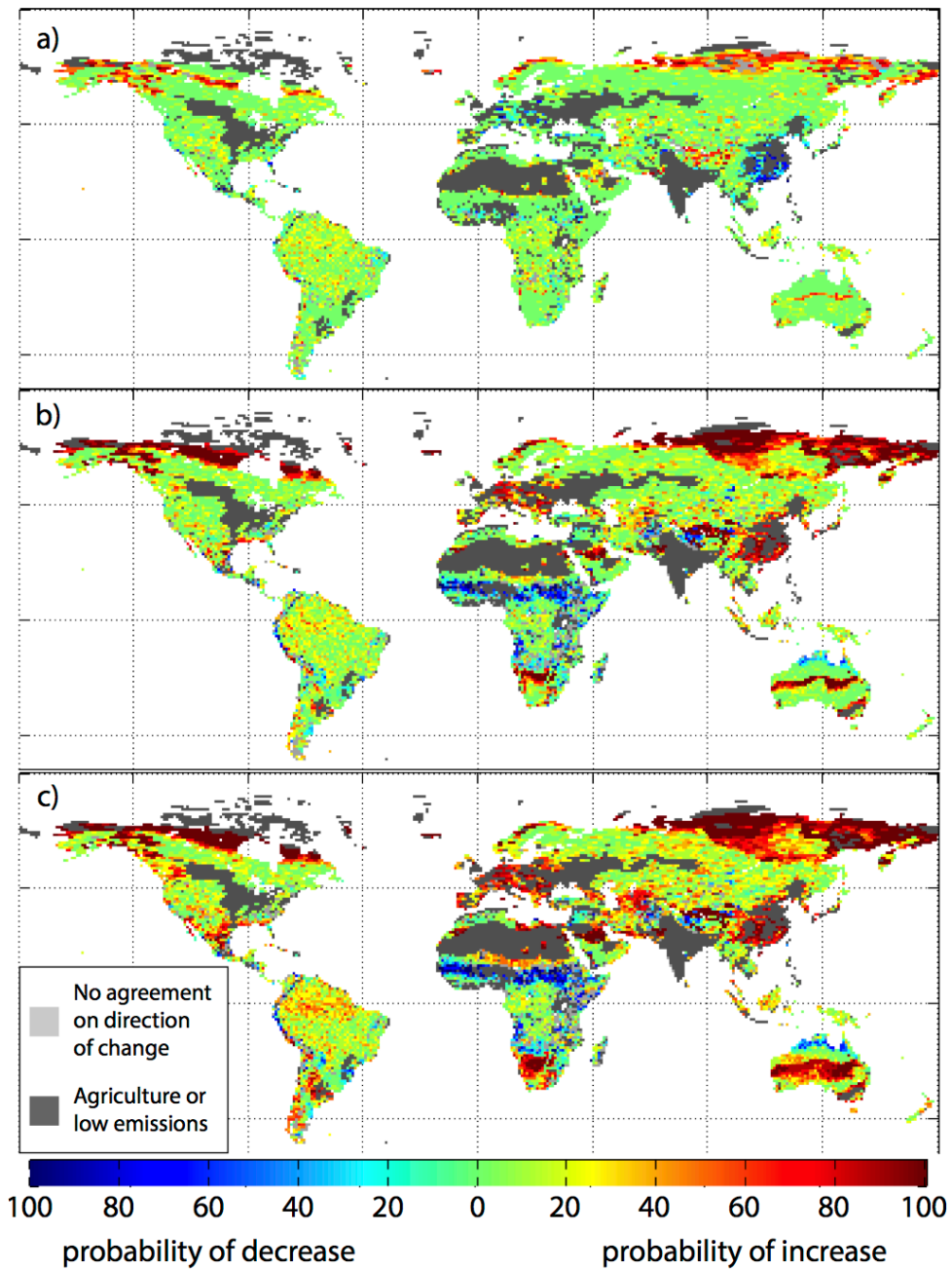
941 *Figure 5: As previous figure, but for average emissions during 1971-2000 and*
 942 *changes as 2071-2100 minus 1971-2000 averages, both differentiated between*
 943 *RCP4.5 and RCP8.5 climate scenarios. In this case, the ensemble is across eight*
 944 *ESMs times five population scenarios.*

945



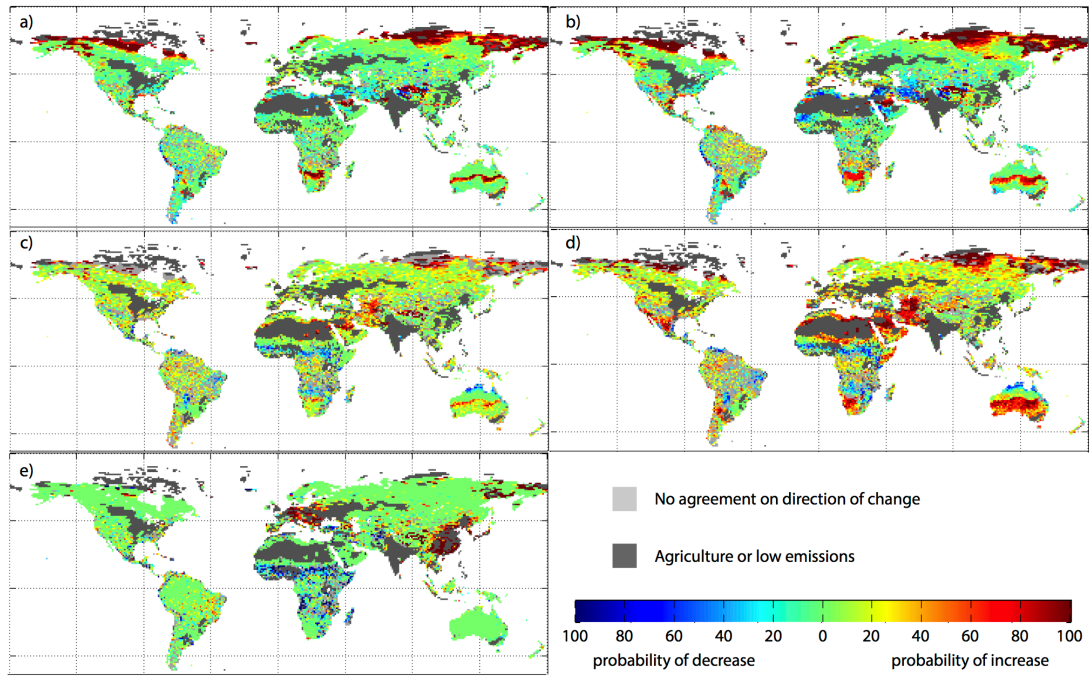
946

947 *Figure 6: Ensemble-mean combustible fuel load in kgC/m² and change due to climate*
 948 *and CO₂ effects. a) Average emissions 1971-2000; b) change from 1971-2000 to*
 949 *2071-2100 for RCP8.5 due to climate effect; c) same as b) but due to CO₂ effect. Grey*
 950 *areas have no fire or are excluded as dominated by agriculture. Combustible fuel*
 951 *load is the amount of carbon potentially emitted if a fire occurs.*



952

953 *Figure 7: Fraction of ensemble members with either a significant decrease or*
 954 *increase in wildfire emissions (positive or negative change by more than two standard*
 955 *deviations of the interannual variability of the initial period); Agricultural areas and*
 956 *areas with ensemble median emissions less than 10% of global median during 2071-*
 957 *2100 were excluded. a) Changes from 1901-1930 to 1971-2000; b) changes from*
 958 *1971-2000 to 2071-2100 for RCP4.5; c) as b) but for RCP8.5.*



959

960 *Figure 8: As previous figure, but for emissions changes due to single driving factors.*

961 *a, b) climate effect, c, d) CO₂ effect, e) population effect; a, c) RCP4.5, b, d) RCP8..*

914 Table 3: Changes in climatic and vegetation fire risk*

<i>Mean annual-maximum Nesterov index</i>												
Region	1901-1930			1971-2000			RCP4.5 ⁽¹⁾			RCP8.5 ⁽¹⁾		
North America	153	(143,	165)	160	(148,	170)	204	(178,	236)	250	(211,	327)
Europe	80	(73,	93)	83	(77,	87)	120	(94,	152)	166	(103,	228)
North Asia	146	(142,	154)	149	(144,	155)	188	(163,	220)	227	(185,	292)
Middle East	2878	(2731,	3184)	2923	(2831,	3169)	3201	(2962,	3443)	3401	(3060,	3776)
South America	240	(223,	254)	248	(233,	272)	298	(258,	338)	348	(265,	432)
Africa	1461	(1379,	1491)	1481	(1434,	1530)	1618	(1519,	1728)	1719	(1566,	1898)
South Asia	288	(272,	314)	296	(276,	318)	332	(300,	368)	368	(312,	449)
Oceania	570	(509,	605)	586	(535,	625)	671	(553,	851)	795	(598,	1085)
Globe	726	(700,	765)	740	(715,	773)	827	(767,	878)	903	(817,	1007)
<i>Grass fraction</i>												
North America	30%	(28%,	31%)	28%	(27%,	29%)	22%	(20%,	23%)	20%	(19%,	22%)
Europe	14%	(13%,	15%)	12%	(11%,	13%)	10%	(9%,	12%)	11%	(9%,	12%)
North Asia	36%	(34%,	37%)	33%	(33%,	34%)	21%	(17%,	23%)	16%	(13%,	18%)
Middle East	75%	(74%,	76%)	76%	(75%,	77%)	77%	(76%,	79%)	76%	(75%,	78%)
South America	26%	(25%,	28%)	23%	(23%,	24%)	16%	(15%,	16%)	13%	(12%,	14%)
Africa	57%	(56%,	59%)	53%	(53%,	54%)	40%	(39%,	42%)	34%	(32%,	36%)
South Asia	26%	(25%,	27%)	23%	(23%,	24%)	17%	(16%,	18%)	15%	(14%,	15%)
Oceania	82%	(79%,	85%)	81%	(79%,	83%)	76%	(74%,	81%)	69%	(65%,	76%)
Globe	43%	(43%,	44%)	41%	(41%,	41%)	33%	(32%,	34%)	29%	(28%,	31%)

* Mean across 8-ESM ensemble, ensemble minimum and maximum in parentheses.

⁽¹⁾ Temporal average for 2071-2100.

915 **Figures**

916 *Figure 1: Simulated global wildfire emissions 1900 to 2100. Shaded areas are for the*
917 *range of ensemble members either across all ESMs using only the central population*
918 *scenario SSP2, or across ESMs and all population scenarios. Lines show ensemble*
919 *averages for specific population scenarios. a) RCP4.5 greenhouse gas concentrations*
920 *and climate change; b) RCP8.5.*

921 *Figure 2: Effects of different factors on global emissions for historical change (until*
922 *2005) and two future climate change scenarios (RCP4.5 and RCP8.5). a) Effect of*
923 *climate change, b) effect of changing atmospheric CO₂, c) effect of changing human*
924 *population density. All simulations are for the central SSP2 population scenario.*
925 *Solid lines for ESM ensemble means and shaded areas for the range across eight*
926 *ESM simulations each.*

927 *Figure 3: Impact of changing fire model parameterisation on the simulated climate,*
928 *CO₂ and population effects on emissions. Standard parameterisation of SIMFIRE*
929 *optimised against GFED3 burned area, optimisation against MCD45 burned area,*
930 *and simulation assuming an increasing effect of population density on burned area*
931 *between 0 and 0.1 inhabitants / km². a) RCP4.5. b) RCP8.5.*

932 *Figure 4: Regional wildfire emissions during 1901-1930 for eight regions and global*
933 *and regional changes, average 1971-2000 minus average 1901-1930, for ensemble*
934 *mean (white/coloured bars) and range across ensemble comprising eight ESMs (error*
935 *bars), in TgC/yr. The change in emissions is further subdivided into climate effect due*
936 *to changes in burned area or changes in combusted fuel per burned area, effect of*

937 atmospheric CO₂ change due to changed burned are or fuel combustion, and
938 population effect.

939 Figure 5: As previous figure, but for average emissions during 1971-2000 and
940 changes as 2071-2100 minus 1971-2000 averages, both differentiated between
941 RCP4.5 and RCP8.5 climate scenarios. In this case, the ensemble is across eight
942 ESMS times five population scenarios.

943 Figure 6: Ensemble-mean combustible fuel load in kgC/m² and change due to climate
944 and CO₂ effects. a) Average emissions 1971-2000; b) change from 1971-2000 to
945 2071-2100 for RCP8.5 due to climate effect; c) same as b) but due to CO₂ effect. Grey
946 areas have no fire or are excluded as dominated by agriculture. Combustible fuel
947 load is the amount of carbon potentially emitted if a fire occurs.

948 Figure 7: Fraction of ensemble members with either a significant decrease or
949 increase in wildfire emissions (positive or negative change by more than two standard
950 deviations of the interannual variability of the initial period); Agricultural areas and
951 areas with ensemble median emissions less than 10% of global median during 2071-
952 2100 were excluded. a) Changes from 1901-1930 to 1971-2000; b) changes from
953 1971-2000 to 2071-2100 for RCP4.5; c) as b) but for RCP8.5.

954 Figure 8: As previous figure, but for emissions changes due to single driving factors.
955 a, b) climate effect, c, d) CO₂ effect, e) population effect; a, c) RCP4.5, b, d) RCP8..